

# An ensemble analysis of climate change impacts on streamflow seasonality across 11 large river basins

S. Eisner<sup>1,2</sup> · M. Flörke<sup>1</sup> · A. Chamorro<sup>3</sup> · P. Daggupati<sup>4</sup> ·  
C. Donnelly<sup>5</sup> · J. Huang<sup>6</sup> · Y. Hundecha<sup>5</sup> · H. Koch<sup>7</sup> ·  
A. Kalugin<sup>8</sup> · I. Krylenko<sup>8,9</sup> · V. Mishra<sup>10</sup> ·  
M. Piniewski<sup>7,11</sup> · L. Samaniego<sup>12</sup> · O. Seidou<sup>13</sup> ·  
M. Wallner<sup>14</sup> · V. Krysanova<sup>7</sup>

Received: 3 February 2016 / Accepted: 21 October 2016 / Published online: 23 January 2017  
© Springer Science+Business Media Dordrecht 2017

**Abstract** The paper investigates climate change impacts on streamflow seasonality for a set of eleven representative large river basins covering all continents and a wide range of climatic and physiographic settings. Based on an ensemble of nine regional hydrological models driven by climate projections derived from five global circulation models under four representative

---

This article is part of a Special Issue on “*Hydrological Model Intercomparison for Climate Impact Assessment*” edited by Valentina Krysanova and Fred Hattermann.

---

✉ S. Eisner  
eisner@usf.uni-kassel.de

<sup>1</sup> Center for Environmental Systems Research, University of Kassel, Kassel, Germany

<sup>2</sup> Present address: Norwegian Institute of Bioeconomy Research, Ås, Norway

<sup>3</sup> Institute of Landscape Ecology, Justus Liebig University, Giessen, Germany

<sup>4</sup> School of Engineering, University of Guelph, Guelph, ON, Canada

<sup>5</sup> Swedish Meteorological and Hydrological Institute, Norrköping, Sweden

<sup>6</sup> Xinjiang Institute of Ecology and Geography, Chinese Academy of Sciences, Xinjiang, China

<sup>7</sup> Potsdam Institute for Climate Impact Research, Potsdam, Germany

<sup>8</sup> Water Problems Institute of RAS, Moscow, Russia

<sup>9</sup> Lomonosov Moscow State University, Moscow, Russia

<sup>10</sup> Civil Engineering, Indian Institute of Technology (IIT) Gandhinagar, Gujarat, India

<sup>11</sup> Warsaw University of Life Sciences, Warsaw, Poland

<sup>12</sup> UFZ-Helmholtz Centre for Environmental Research, Leipzig, Germany

<sup>13</sup> Department of Civil Engineering, University of Ottawa, Ottawa, ON, Canada

<sup>14</sup> Federal Institute for Geosciences and Natural Resources, Hannover, Germany

concentration pathways, we analyzed the median and range of projected changes in seasonal streamflow by the end of the twenty-first century and examined the uncertainty arising from the different members of the modelling chain. Climate change impacts on the timing of seasonal streamflow were found to be small except for two basins. In many basins, we found an acceleration of the existing seasonality pattern, i.e. high-flows are projected to increase and/or low-flows are projected to decrease. In some basins the hydrologic projections indicate opposite directions of change which cancel out in the ensemble median, i.e., no robust conclusions could be drawn. In the majority of the basins, differences in projected streamflow seasonality between the low emission pathway and the high emission pathway are small with the exception of four basins. For these basins our results allow conclusions on the potential benefits (or adverse effects) of avoided GHG emissions for the seasonal streamflow regime.

## 1 Introduction

Most streamflow regimes feature a distinct seasonality, i.e., a characteristic timing and magnitude of high-flow and low-flow periods, resulting from local seasonal cycles of precipitation, evaporation demand, and snow accumulation and melt (Dettinger and Diaz 2000). Expected climate change may alter the seasonal streamflow regime in many regions through a variety of (potentially interfering) mechanisms including shifts in the temporal and spatial precipitation pattern, changes in snow-melt timing due to rising temperature, or increasing evaporation demand. Regional impacts of climate change on streamflow seasonality have been addressed in a large body of studies by driving *one* regional hydrological model (HM) with ensemble climate projections in a set of river basins (Beldring et al. 2008; Jung et al. 2013; Addor et al. 2014; Aich et al. 2014; Morán-Tejeda et al. 2014; Vano et al. 2015). In very rare cases, an ensemble of climate projections *and* HMs has been applied to study climate change impacts on streamflow regimes in a single river basin (Cornelissen et al. 2013) or several river basins (Vetter et al. 2015), mainly because setting up and calibrating several HMs in the single basins is significantly more time and resource consuming. The results and insights gained from individual regional studies, however, are difficult to compare and to synthesize across regions because the single modelling studies differ substantially in study setup concerning one or several of the following aspects: (1) the general circulation model and/or regional climate model used, (2) the bias-correction method(s) applied to the climate forcing, (3) the emission scenario(s) considered, (4) the hydrological model(s) applied, and (5) the time period analyzed (near-future vs. long-term).

Continental to global scale impact assessments can be provided by macro-scale hydrological models (global hydrological models or land surface models) which are increasingly used in a model-ensemble manner to examine global change and climate change impacts on hydrological regimes (Hagemann et al. 2013; Prudhomme et al. 2014; Schewe et al. 2014; Haddeland et al. 2014). The advantage of global coverage, however, comes at the expense of a coarser spatial resolution, less detailed process representation and limited or no possibility of regional parameter adjustment (Bierkens 2015; Greuell et al. 2015) which can impact the accuracy of their simulations.

As part of the Intersectoral Impact Model Intercomparison Project (ISI-MIP, Warszawski et al. 2014), this study aims to overcome the fragmentarity of previous regional-scale hydrologic

impact assessments by applying nine regional hydrological models in eleven representative river basins covering all continents and a wide range of climatic and physiographic settings. Based on an ensemble of bias-corrected climate projections from five global circulation models (GCMs) under four representative concentration pathways (RCPs), we comprehensively examine climate change impacts on streamflow seasonality by the end of the twenty-first century and investigate the sources of uncertainty in projected seasonal streamflow.

## 2 Material and methods

**River basins and multi-model ensemble** Eleven representative large river basins were chosen to study climate change impacts on streamflow seasonality. The basin set includes Rhine and Tagus in Europe, upper Amazon in South America, upper Mississippi in North America, Lena, Ganges, upper Yellow, and upper Yangtze in Asia, Blue Nile and Niger in Africa, and Darling in Australia. Depending on the basin, up to nine regional hydrological models (HMs) were forced using the bias-corrected outputs of five GCMs (HadGEM2-ES, IPSL-CM5A-LR, MIROC-ESM-CHEM, GFDL-ESM2M, NorESM1-M) under four RCPs (RCP2.6, RCP4.5, RCP6.0, RCP8.5) to provide streamflow projections for the twenty-first century; however the number and set of HM outputs available varies between basins. The list of HMs available per basin is provided in Table 1. The main characteristics of the eleven study basins as well as of all participating HMs are provided in the editorial to this special issue. All HMs were calibrated to twentieth century observed discharge in the individual basins. The general calibration approach was not harmonized between models, i.e. optimisation algorithm, objective function as well as the number and type of calibrated parameters vary between models. Model performance for various streamflow characteristics has been evaluated by Huang et al. (2016) for all HMs and river basins considered in this study. According to all possible GCM and RCP combinations, each HM provided 20 transient hydrologic projections covering the time period 1971–2099. For a detailed description of the driving data-set and the bias-correction method, readers are referred to Hempel et al. (2013). Hydrological projections were derived as natural discharge, i.e., the simulations do not account for human interference on the natural flow regime through e.g., flow regulation and water abstraction, with two exceptions: The SWIM simulations in the Tagus basin and the SWAT simulations in the Niger include flow regulation by reservoirs.

**Processing** Analyses were based on streamflow climatologies, i.e. long-term average monthly streamflow in the individual basins. Projected daily streamflow from the multi-model ensemble was aggregated by arithmetic averaging to monthly climatologies and analyzed for two 30-year periods representing the present-day (1981–2010) and end-century conditions (2070–2099). To be able to compare streamflow between basins, streamflow values were normalized by catchment area into specific flows, i.e., in millimeters per unit of time (either month or year). Relative and absolute changes between present-day and future conditions were calculated for the respective GCM baseline (1981–2010) to avoid artefacts caused by possible systematic offsets among the GCM baselines as well as between GCM baselines and present-day observed climate conditions.

**Uncertainty analysis** To quantify the contribution of GCMs, RCPs, and HMs to the total uncertainty in simulated present-day and projected end-century streamflow climatologies, the isolated shares of these three distinct sources on total ensemble variance were calculated

**Table 1** River basin set and available models in the individual basins. Asterisks represent the number of simulations available for each hydrological model and basin

Basin	Rhine	Tagus	U. Niger	Blue Nile	Ganges	U. Yellow	U. Yangtze	Lena	Darling	U. Mississippi	U. Amazon
Gauge	Lobith	Almourol	Koulikoro	El Deim	Farakka	Tangnathal	Cuntan	Stolb	Louth	Alton	SP Olivenca
Drainage area, km <sup>2</sup>	160,800	67,490	120,000	238,977	835,000	121,000	804,859	2,460,000	489,300	444,185	990,781
Average T, deg. C	8.7	14	26.5	19.4	21.1	-2	6.8	-10.2	19.2	7.3	21.7
Average P, mm/yr	1038	671	1495	1405	1173	506	768	384	590	967	2122
ECOMAG				*				*			
HBV	**	*	*	*	*	*	*			*	*
HYMOD	**		*		**	*			*	**	*
HYPE	*	*			*			*			
mHM	*		*	*	*	*			*	*	*
SWAT			*	*	*		*		*	*	*
SWIM	*	*	*	*	*	*	*	*	*	*	*
VIC	*	*	*	*	*	*	*	*	*	*	*
WaterGAP3	*	*	*	*	*	*	*	*	*	*	*

according to the method proposed by Hawkins and Sutton (2009) which was applied in various hydrologic impact studies (Wada et al. 2013; Arnell and Gosling 2013; Arnell and Lloyd-Hughes 2014). Given the assumption that the three sources of uncertainty are independent—hence uncorrelated—the uncertainty attributable to GCMs ( $V_{GCM}$ ) was estimated by (1) calculating the variance in simulated streamflow over all GCMs for a given HM-RCP combination, (2) repeating this exercise for all remaining HM-RCP combinations, and (3) averaging the variances derived from the single HM-RCP combinations. This procedure was repeated analogously to estimate the variance across HMs ( $V_{HM}$ ) and RCPs ( $V_{RCP}$ ). The total variance  $V_t$  of the ensemble is given by the sum of the isolated sources as

$$V_t = V_{GCM} + V_{RCP} + V_{HM}$$

### 3 Results

#### 3.1 Climate change impacts on streamflow seasonality

In order to quantify climate change impacts on the magnitude of streamflow seasonality, i.e., the degree to which the annual streamflow volume is concentrated on certain months, Table 2 lists the seasonality index SI (Walsh and Lawler 1981) of the multi-model ensemble median for present-day climate and end-century climate under RCP2.6 and RCP8.5. SI theoretically ranges between 0 (streamflow equally distributed over all months) and 1.2 (entire streamflow volume discharges in only one month). Changes in SI between present-day and end-century conditions are generally small, with the exception of Rhine and Darling. Under RCP8.5, both basins show considerably higher SI values compared to present-day, i.e. annual streamflow volume is more strongly concentrated in the high-flow season.

Ensemble median monthly streamflow climatologies for present-day and end-century conditions under RCP2.6 and RCP8.5 are shown in Fig. 1. This figure synthesizes the

**Table 2** Seasonality index (SI) of ensemble median streamflow climatologies for present-day and projected end-century conditions under RCP2.6 and RCP8.5. Minimum and maximum values in the ensemble of HM-GCM combinations are shown in brackets

Basin	present-day	RCP 2.6	RCP 8.5
Rhine	0.19 (0.13–0.28)	0.21 (0.16–0.27)	0.31 (0.15–0.41)
Tagus	0.55 (0.41–0.87)	0.56 (0.39–0.94)	0.51 (0.41–0.90)
Blue Nile	0.86 (0.76–1.06)	0.85 (0.69–1.07)	0.85 (0.63–1.05)
Niger	0.91 (0.64–1.04)	0.93 (0.66–1.06)	0.92 (0.67–1.11)
Lena	0.75 (0.69–0.89)	0.76 (0.61–0.89)	0.72 (0.55–0.84)
Up. Yangtze	0.72 (0.59–0.78)	0.72 (0.60–0.79)	0.73 (0.62–0.79)
Up. Yellow	0.64 (0.51–0.76)	0.64 (0.55–0.79)	0.66 (0.53–0.87)
Ganges	0.91 (0.61–1.11)	0.93 (0.63–1.15)	0.96 (0.63–1.18)
Darling	0.49 (0.26–0.78)	0.44 (0.13–0.83)	0.73 (0.24–1.09)
Up. Amazon	0.21 (0.18–0.31)	0.22 (0.17–0.33)	0.24 (0.15–0.41)
Up. Mississippi	0.33 (0.21–0.50)	0.31 (0.18–0.50)	0.34 (0.21–0.66)

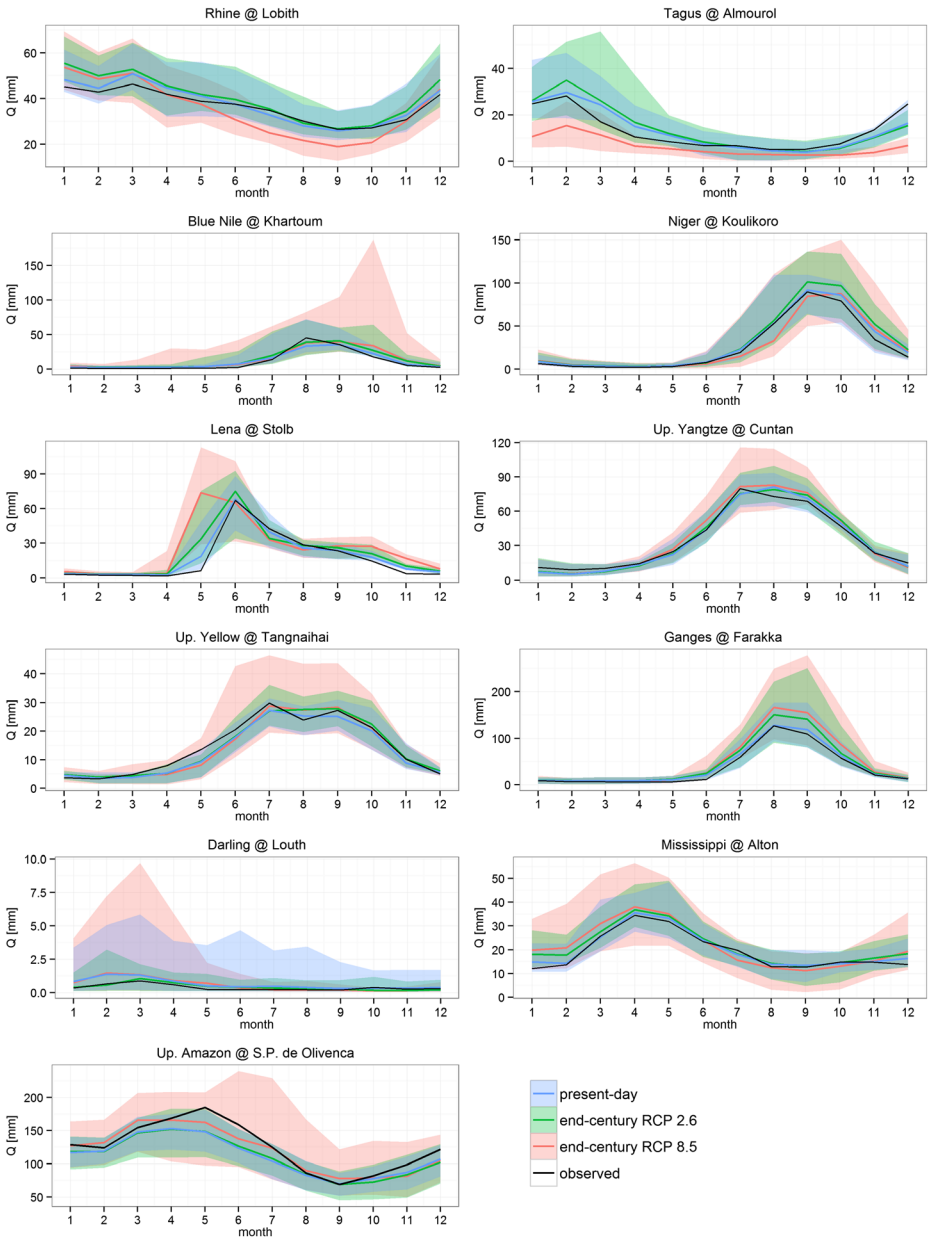


**Fig. 1** Projected monthly streamflow climatologies for present-day (1981–2010) and end-century (2070–2099) conditions. Solid lines show the ensemble median of all GCM-HM combinations, shades cover the 5th to 95th percentile range. The twentieth century observed streamflow climatology is shown in black

results derived from all possible GCM-HM combinations for each of the two RCPs, thus also illustrates the uncertainty ranges associated with the projected streamflow climatology in the various basins. Note that the sample size varies between 20 and 45 simulations depending on the number of available HMs in the individual basins. Figure 2

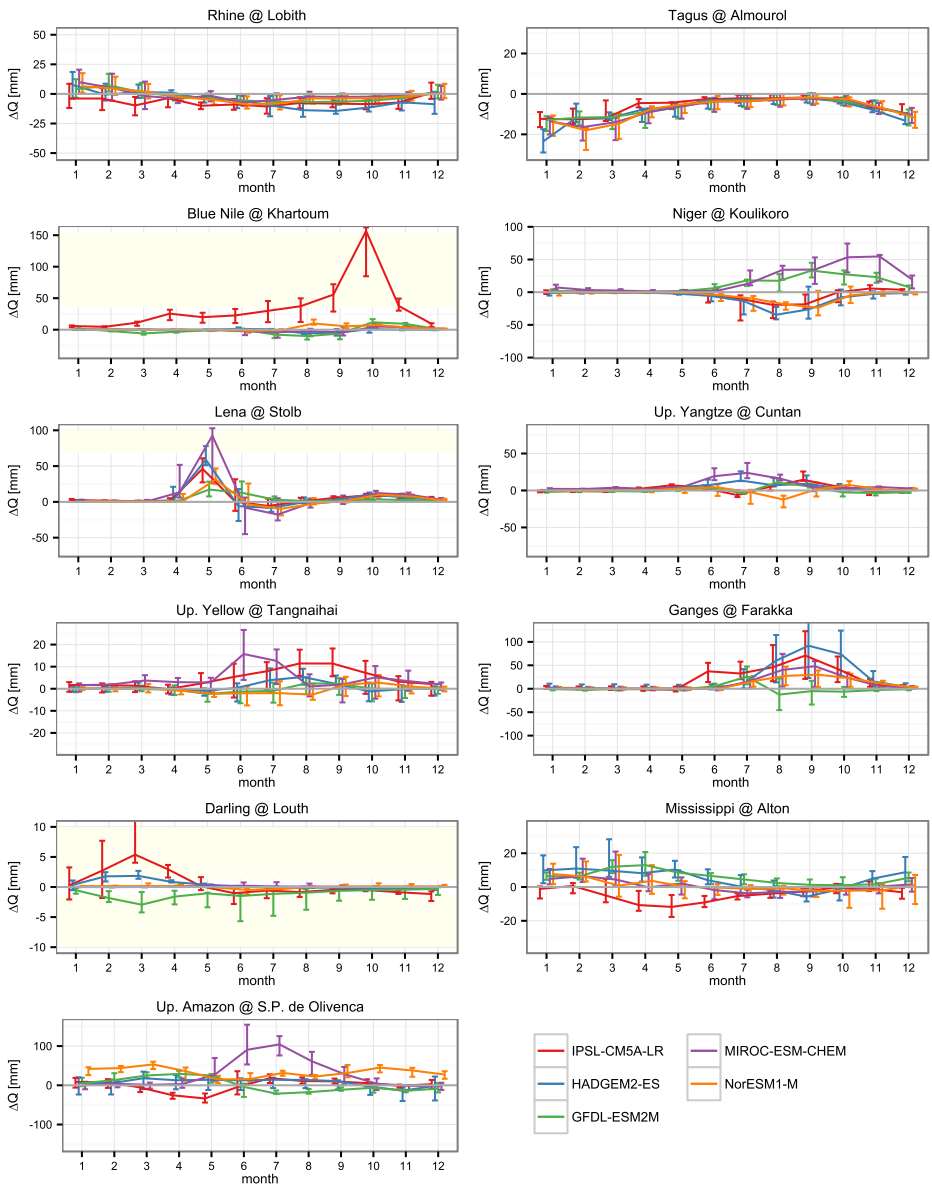


**Fig. 2** Projected absolute change in streamflow climatology shown for RCP8.5 and the period 2070–2099, separately plotted for each GCM. Error bars show the range between hydrological models. By default, y-axes extend to  $\pm$  the range of the present-day climatology; beige shading highlights plotting regions outside this default range

provides the medians and ranges of projected changes in monthly streamflow under RCP8.5, separately shown for the single GCMs. Projected changes under RCP2.6 are shown in Fig. 3. In the following, impacts of climate change on streamflow climatology as visualized in Figs. 1–3 are separately described for the eleven river basins.

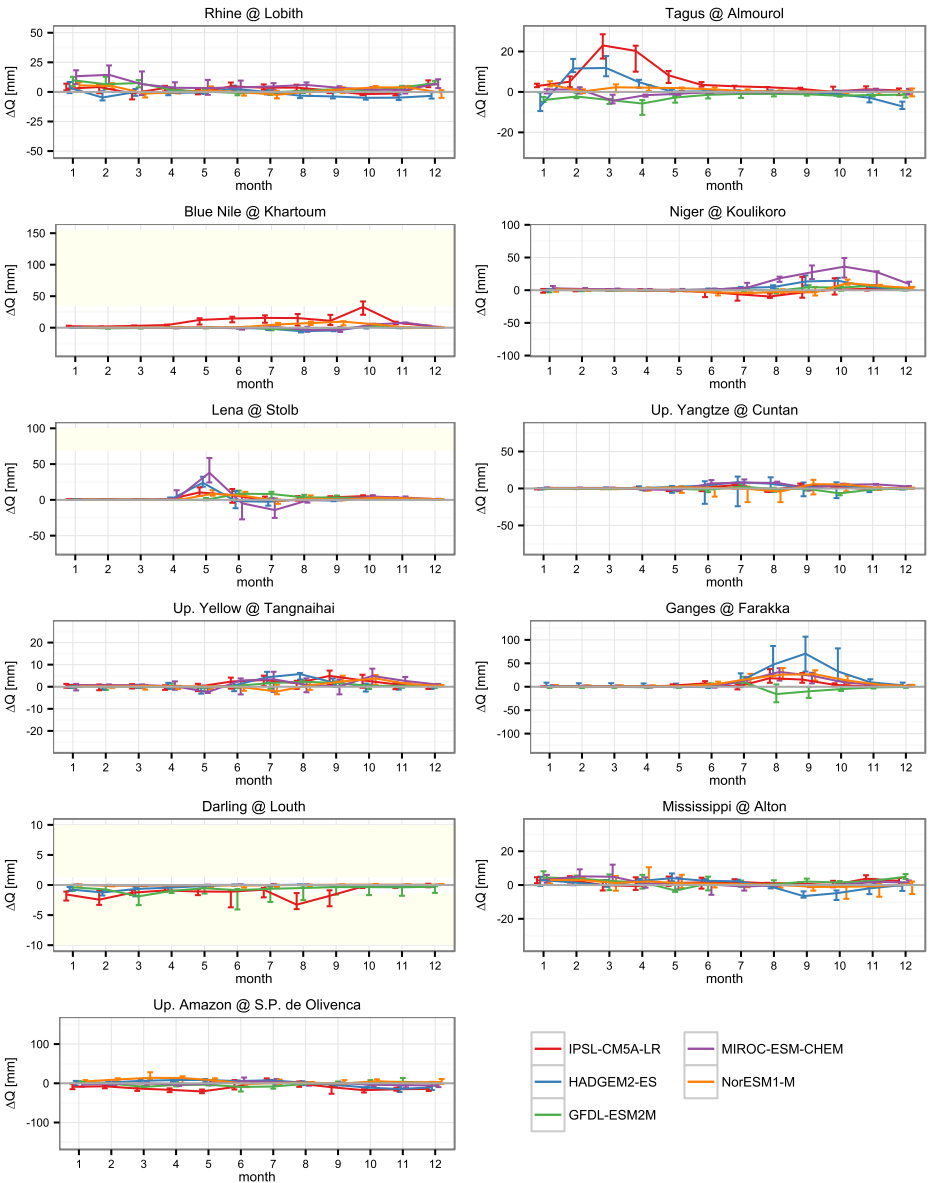


**Fig. 3** Projected absolute change in streamflow climatology shown for RCP2.6 and the period 2070–2099, separately plotted for each GCM. Error bars show the range between hydrological models. By default, y-axes extend to  $\pm$  the range of the present-day climatology; beige shading highlights plotting regions outside this default range

### 3.1.1 Rhine

Compared to most other basins considered in this study, the lower Rhine features a rather uniform seasonal streamflow regime with a high-flow period in winter and early spring. Under



RCP8.5 streamflow seasonality is projected to intensify in that winter high flows increase and summer low flows decrease. Ensemble median change by the end of the century ranges between  $-7$  mm ( $-27$  %) in September and  $+5$  mm ( $+10$  %) in January. While the decrease in summer and autumn flows is consistently projected by the majority of GCM-HM combinations, streamflow response in the winter period (December to February) is rather uncertain with decreases and increases visible depending on the GCM (cf. Fig. 2). Under RCP2.6, median streamflow volumes remain unchanged in the summer low-flow period while winter high-flows are projected to increase, especially between December and February by in total  $+17$  mm ( $+12$  %) (Fig. 3).

### 3.1.2 Tagus

In the Tagus basin, all GCM-HM combinations consistently project a substantial reduction in streamflow volumes in the high-flow season (December to March) under RCP8.5. The cumulative reduction of streamflow volume in these months amounts to  $-56$  mm ( $-55$  %). While in absolute terms the reduction in streamflow is highest during the high-flow season, it is noteworthy that under RCP8.5 the multi-model ensemble consistently projects decreasing streamflow in all months of the year (Fig. 2) attributable to both a significant decrease of average annual precipitation ( $-27.3$  %) and a general increase in evapotranspiration due to temperature increase (Mishra et al., this issue). In contrast, climate change impacts on streamflow seasonality are smaller under RCP2.6. Based on the multi-model median, streamflow volume is projected to increase by  $+4$  mm ( $+13$  %) in February and remains practically unchanged in the remaining months. Despite the fact that the multi-model median indicates only small changes, Fig. 3 shows that the simulations driven by IPSL-CM5-LR and HADGEM2-ES result in considerable increases in streamflow between February and April under RCP2.6 (Fig. 3).

### 3.1.3 Blue Nile

Judged from the ensemble median, climate change impacts on streamflow seasonality in the Blue Nile basin are small. Under RCP8.5, annual streamflow volume is projected to increase by  $+24$  mm ( $+16$  %); the largest absolute increase occurs at the end of the rain season in October ( $+11$  mm) corresponding to approximately  $50$  % of the total annual streamflow increase. Under RCP2.6, annual streamflow is projected to increase by  $+28$  mm ( $+20$  %) with  $90$  % of the additional streamflow being discharged in the high-flow season between July and November (cf. also Fig. 3). Figure 2 illustrates, however, that the hydrological simulations based on IPSL-CM5A-LR forcing under RCP8.5 result in huge streamflow increases in all months caused by a comparable increase in precipitation in particular at the end of the rain season (August to October). To what extent the surplus precipitation translates into increasing streamflow volumes varies considerably between the individual HMs. Total simulated increases summed up for the three-month period ranges between  $+256$  mm and  $+475$  mm compared to present-day conditions.

### 3.1.4 Niger

In the Niger basin, the ensemble median shows decreasing streamflow at the beginning of the wet season under RCP8.5 with the largest reduction of  $-22$  mm ( $-37$  %) occurring in August.

Under RCP2.6 streamflow volume is projected to increase in the high-flow season with largest increases found in September and October which substantially contribute to an overall increase in annual streamflow volume of +30 mm (+8 %) (Fig. 3). Figure 1 illustrates that the uncertainty range of GCM-HM combinations around the ensemble median substantially increases when moving from present-day climate to future conditions which is mainly caused by inconsistent directions of change derived from the GCM ensemble (shown in Fig. 2 for RCP8.5). This results in uncertainty in the timing of the peak flow period in future climates. The hydrological simulations based on GFDL-ESM2M and MIROC-ESM-CHEM forcing consistently indicate increasing streamflow volumes in the second half of the year while the remaining simulations indicate decreasing streamflow volumes from July to September. The opposite directions of change derived from individual GCMs offset each other in the ensemble median.

### 3.1.5 Lena

The Lena streamflow regime is generally dominated by a strong snowmelt peak in June. Figure 1 shows that the maximum monthly discharge is projected to shift from June to May under RCP8.5 which is most likely related to an earlier onset of snowmelt due to rising average temperatures (+7.1 K). Annual precipitation in the basin is projected to increase on average by 30 % under RCP8.5 and by 10 % under RCP2.6 translating into a median increase in annual streamflow of +94 mm and +51 mm, respectively. Although the strongest precipitation increase occurs in autumn, about 70 % of the additional streamflow volume is discharged in May and June. This implies that climate change increases total snow accumulation in the winter season and explains the amplification of the snowmelt flood visible for both RCPs.

### 3.1.6 Upper Yangtze

Streamflow seasonality in the upper Yangtze basin is dominated by monsoonal rainfall with annual high flows occurring between June and October. While the general seasonality remains unaffected by climate change, the multi-model median projects increases in streamflow volume between June and October under RCP8.5 resulting in a slight increase in annual streamflow volume of +27 mm (+6 %). Four out of five GCMs result in increased streamflow volumes in the monsoon season with the largest overall increase in wet-season streamflow volume found for MIROC-ESM-CHEM (Fig. 2), yet the change pattern within the wet season strongly depends on the underlying GCM. Figure 1 illustrates, however, that the uncertainty in projected streamflow—as indicated by the multi-model range—is particularly large in the monsoon season. Under RCP2.6 median monthly streamflow volumes remain at present-day levels.

### 3.1.7 Upper Yellow

Streamflow seasonality in the upper Yellow basin is found to be largely unaffected by climate change. The ensemble median shows a moderate increase in streamflow volume in the high-flow season (July to September) amounting to +8 mm (+10 %) for RCP8.5 and to +4 mm (+5 %) for RCP2.6 (Fig. 1). Overall, this increase originates from two GCMs: hydrological projections based on MIROC-ESM-CHEM result in higher streamflow in the beginning of the wet season (June and July) while projections based on IPSL-CM5A-LR show increased

streamflow values especially at the end of the wet season (August and September). Streamflow projections based on the remaining three GCMs show only minor deviations from present-day conditions (cf. Figure 2 and Fig. 3).

### 3.1.8 Ganges

Streamflow seasonality in the Ganges basin is determined by both monsoon-dominated rainfall and snowmelt from the Himalaya. While the general seasonality pattern at the Farakka gauge remains unaffected by climate change, the multi-model ensemble projects considerable increases in streamflow in the high-flow season from July to October (Fig. 1). Based on the ensemble median, annual streamflow volume increases by +125 mm (+26 %) under RCP8.5 and +77 mm (+16 %) under RCP2.6. For both RCPs, around 90 % of the additional streamflow volume is discharged between July and October. Figures 2 and 3 illustrate that this change signal is consistently found across GCMs: four out of five GCMs result in increasing streamflow volumes in the high-flow season caused by a substantial increase in precipitation in the monsoon season. Although there is a broad agreement in the direction of change, large uncertainty is found in the actual amplitude arising from both HMs and GCMs.

### 3.1.9 Darling

The semi-arid Darling basin features the smallest runoff ratio in the basin set with ensemble median monthly streamflow ranging between 0.3 mm and 1.2 mm. Figure 1 highlights that the streamflow estimates for both present and future conditions are associated with substantial uncertainty as indicated by the 5th–95th percentile range. Under RCP8.5, streamflow volumes tend to further decrease in the low-flow period between May and December. During the wet season (January to April), the climate change related streamflow signal is inconclusive with increases, decreases and stable conditions found depending on the GCM (Fig. 2). Under RCP2.6 the majority of GCM-HM combinations projects unchanged or decreasing streamflow throughout the year resulting in a decrease in ensemble-median annual streamflow volume of  $-2.5$  mm ( $-33$  %) (Fig. 3).

### 3.1.10 Upper Mississippi

Projected changes in streamflow seasonality in the upper Mississippi are generally small when only the ensemble median is considered (Fig. 1). Streamflow volumes are projected to moderately increase between December and April by in total + 25 mm (+24 %) under RCP8.5 and by +11 mm (+11 %) under RCP2.6. Figure 2 reveals that the hydrological projections disagree in the direction of change particularly between March and June with decreases, increases and unchanged conditions found depending on the GCM the simulation is based on. Note that despite the fact that the ensemble median changes under RCP8.5 are small, a large spread in projected changes is found, in particular between January and June.

### 3.1.11 Upper Amazon

Based on the multi-model ensemble median, climate change impacts on streamflow seasonality remain small in the upper Amazon basin. Under RCP8.5, annual precipitation is projected to increase by on average 11.3 % which translates into small to moderate increases in monthly

streamflow volumes (between +8 mm and +19 mm) throughout the year with the exception of the period from October to December. It becomes clear from Fig. 2, however, that this small median effect mainly results from opposite climate change signals from the driving GCMs cancelling in the ensemble median. Monthly change patterns differ substantially depending upon the GCM considered. This observation is further corroborated by the large uncertainty range around the ensemble median streamflow. Under RCP2.6, the ensemble median streamflow climatology largely follows the present-day climatology, it can thus be concluded that climate change impact on streamflow seasonality remains neglectable. Figure 3 illustrates that, depending on GCM and HM, small increases or decreases in streamflow volume are projected with no consistent direction of change.

### 3.2 Uncertainty in streamflow climatologies

In the previous section, we chose the ensemble median as a robust estimator to analyze climate change impact on streamflow seasonality. It has, however, also been shown that the streamflow projections are associated with substantial uncertainty as indicated by the 5th–95th percentile ranges displayed in Fig. 1. Figure 4 shows total uncertainty in projected streamflow climatologies at the end of the twenty-first century split into the distinct sources GCM, RCP and HM. For reference, variability in simulated present-day streamflow climatologies is also shown which arises from hydrological model uncertainty (differences between the HMs regarding model structure and parametrization) as well as from remaining biases between GCM base-lines (which were consistently bias-corrected to WATCH forcing data). Total uncertainty (i.e., variance) in each month and period was normalized by the maximum value found in individual basins.

In all basins, uncertainty in monthly streamflow climatologies substantially increases when moving from present-day conditions to the end-century projection. It is noteworthy that in most basins HM contribution to total uncertainty by end-century is similar to that in the baseline period, i.e., the increase in total uncertainty is driven by GCMs and RCPs. In basins where the individual GCMs resulted in an inconsistent direction of change (increase, unchanged, or decreasing streamflow depending on the GCM), GCMs consequently constitute the largest share to total uncertainty, e.g., apparent in the Ganges, Niger, Upper Amazon, and Upper Yellow. A considerable contribution of RCPs to total uncertainty is found for the Tagus (high-flow season), Rhine (esp. low-flow season), and Lena (snow melt onset in May/June).

## 4 Discussion and conclusions

Based on a multi-model ensemble, we studied the impact of climate change on seasonal streamflow using the example of eleven representative large river basins covering all continents and a wide range of climatic and physiographic settings.

In the majority of the study basins, climate change was found to have no or only a small effect on the temporal pattern of streamflow, i.e., the timing of high-flow and low-flow periods, with the exception of Lena and Niger. The main phase of streamflow in the Lena basin, as well as in other arctic rivers, is spring-summer snow melting, which is sensitive to warming within these seasons. Projected increases in air temperatures in the northern latitudes lead to advancing of the snowmelt season, and as result to an earlier

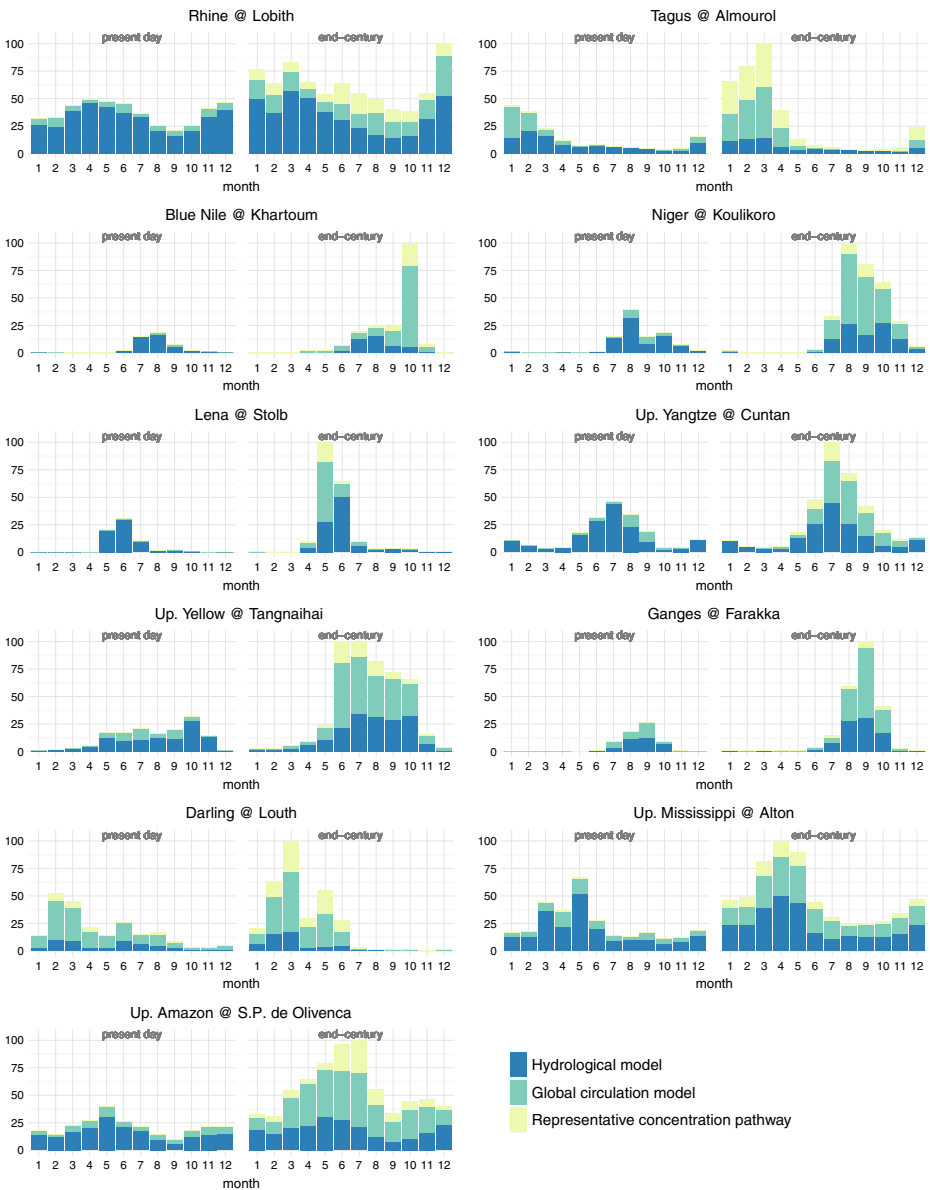


**Fig. 4** Uncertainty in simulated present-day streamflow climatologies and projected end-century streamflow climatologies split into the three distinct sources HM, GCM, and RCP. Results were scaled (divided) by maximum variability to show the temporal evolution of the overall uncertainty

beginning of the flood season of the northern rivers. This effect was also reported in the studies by Gelfan et al. (2016), Krylenko et al. (2015), and Schneider et al. (2013), among others. In the Niger basin we found a substantial reduction of streamflow volume in August under RCP8.5, i.e., the beginning of the high-flow season is projected to shift by one month from August to September. This result corresponds well with modelling

studies concluding a later start of the wet season over the semi-arid African Sahel due decreasing precipitation amounts in July and August (Biasutti and Sobel 2009; Patricola and Cook 2010). It has to be noted that the temporal scale of our analysis (monthly) limits our conclusions to shifts of at least one month. Some basins may feature shifts in seasonality at sub-monthly time scales that could not be identified within the current study design.

Climate change was found to have a substantial impact on the magnitude of streamflow seasonality (as quantified by SI) in only two out of eleven river basins, Rhine and Darling. In both basins seasonality intensified under end-century climate conditions. At the same time, streamflow projections in the Darling have been shown to exhibit tremendous uncertainty for both present-day conditions and future projections, which may be related to the fact that the (present-day) streamflow regime is characterized by considerable inter-annual to decadal variability as well as to the very low runoff coefficient (cf. Table 1 in the editorial of this Special Issue). To arrive at more conclusive results on climate change impact on the streamflow regime in the Darling basin, as well as in similar basins, an analysis based on flow quantiles rather than seasonal cycles might be more expedient.

Despite the small quantifiable effect on the magnitude of streamflow seasonality (with respect to SI), our results show that climate change leads to an amplification of the existing seasonality pattern in many basins:

- All basins influenced by monsoonal precipitation (Ganges, Yangtze, Yellow) consistently show increased streamflow volumes during the high-flow season, although the distinctiveness of this signal varies between basins. This finding is closely linked to the intensification of northern hemisphere summer monsoon consistently projected by the majority of the CMIP5 models (Lee and Wang 2012; Menon et al. 2013).
- The multi-model ensemble consistently projects a substantial decrease of annual streamflow volume in the Tagus basin with decreasing streamflow in all months under RCP8.5.
- In the Lena basin increased snow accumulation leads to an amplification of the snow-melt flood peak.
- In the Rhine basin, the multi-model ensemble consistently projects increasing winter streamflow, under RCP8.5 combined with decreasing summer low-flows.

The uncertainty in GCM projected precipitation patterns precludes any robust conclusions on climate change impact on streamflow seasonality in the Amazon, Mississippi, and Niger, the latter except for the beginning of the high-flow season (RCP2.6) as discussed earlier. In these basins, the individual GCM simulations result in distinctly different seasonal change patterns with opposite directions of change (increase versus decrease), i.e., no consistent signal across the different GCMs could be found. The opposite directions of change often cancelled out in the ensemble median which consequently indicated no or only small changes in streamflow seasonality. We chose the ensemble median as a robust estimator to deduce changes in streamflow seasonality from the multi-model ensemble. Our results, however, highlight that the ensemble median is not informative if the different GCMs result in opposite directions of change.

In the majority of the study basins we find that GCM forcing constitutes the largest share to total uncertainty in projected streamflow climatologies, in particular in basins where the

individual GCMs resulted in an inconsistent direction of change. In this respect, our results compare well to and complement the study by Vetter et al. (2016) who analyzed the uncertainty in selected flow signatures (mean annual streamflow,  $Q_{10}$  high-flow, and  $Q_{90}$  low-flow) using the same basin set. The authors concluded that in the majority of the cases GCM uncertainty prevailed, and found considerable contribution of RCPs in the same basins identified in this study (Tagus, Rhine, Lena). While uncertainty due to GCMs and RCPs prevails by the end of the century in the majority of the basins, HMs are found to constitute a considerable share to total uncertainty, although to varying degree depending on river basin. Similar to Samaniego et al. (2016), we conclude that uncertainty in hydrological projections due to HMs cannot be neglected.

In the majority of the basins, differences in projected streamflow seasonality between the low emission pathway (RCP2.6) and the high emission pathway (RCP8.5) are small; exceptions are the Tagus, Rhine, Niger (onset wet season in August), and Lena. For example, the Tagus basin is projected to experience a substantial reduction in streamflow throughout the year under RCP8.5 due to decreasing precipitation and increasing evaporation while unchanged or slightly increasing streamflow volumes are projected under RCP2.6. For these basins, our results allow conclusions on the potential benefits (or adverse effects) of avoided GHG emissions for the seasonal streamflow regime.

It has to be emphasized that we limited our analysis to climate change impacts on the natural streamflow regime. In many regions of the world, the natural flow regime is already significantly altered by human activity through e.g. flow regulation, water abstraction and transfer, and land-use change (Döll et al. 2009; Grill et al. 2015). Projected population growth and economic development are expected to increase the demand for land and water resources, thus are likely to intensify human interference on the streamflow regime. These direct anthropogenic impacts may exceed the climate-induced alterations analyzed here (Arrigoni et al. 2010; Wang and Hejazi 2011; Patterson et al. 2013; Haddeland et al. 2014).

The study design building on a multi-model and multi-basin ensemble allowed for a comprehensive and consistent analysis of climate change impacts on streamflow seasonality over a wide range of climatic and physiographic settings, i.e. it allowed to contrast and compare expected impacts on streamflow seasonality between regions. At the same time, the study design facilitates a more comprehensive quantification and attribution of uncertainty in streamflow projections (cf. also Vetter et al. in this issue). In this respect, this study overcomes the fragmentarity of most previous regional climate change impact studies addressing streamflow regime and seasonality.

It remains, however, unknown whether our findings for individual basins are representative for larger hydro-climatic regions. Including additional river basins for each hydro-climatic region would be a promising way forward to arrive at more general conclusions and to further substantiate the findings of this study.

**Acknowledgments** This work has been conducted under the framework of ISI-MIP. The ISI-MIP Fast Track project was funded by the German Federal Ministry of Education and Research (BMBF) with project funding reference number 01LS1201A. Responsibility for the content of this publication lies with the authors. We acknowledge the World Climate Research Programme's Working Group on Coupled Modelling, which is responsible for CMIP, and we thank the respective climate modelling groups for producing and making available their model output. We would like to thank all regional-scale water sector modellers who uploaded their modelling results to the ISI-MIP server. We also acknowledge the support of the Global Runoff Data Center. We thank two anonymous reviewers for their valuable suggestions that improved the manuscript significantly.

## References

- Addor N, Rössler O, Köplin N et al (2014) Robust changes and sources of uncertainty in the projected hydrological regimes of Swiss catchments. *Water Resour Res* 50:7541–7562. doi:10.1002/2014WR015549
- Aich V, Liersch S, Vetter T et al (2014) Comparing impacts of climate change on streamflow in four large African river basins. *Hydrol Earth Syst Sci* 18:1305–1321. doi:10.5194/hess-18-1305-2014
- Arnell NW, Gosling SN (2013) The impacts of climate change on river flow regimes at the global scale. *J Hydrol*. doi:10.1016/j.jhydrol.2013.02.010
- Arnell N, Lloyd-Hughes B (2014) The global-scale impacts of climate change on water resources and flooding under new climate and socio-economic scenarios. *Clim Chang* 122:127–140. doi:10.1007/s10584-013-0948-4
- Arrigoni AS, Greenwood MC, Moore JN (2010) Relative impact of anthropogenic modifications versus climate change on the natural flow regimes of rivers in the northern Rocky Mountains, United States. *Water Resour Res* 46:W12542. doi:10.1029/2010WR009162
- Beldring S, Engen-Skaugen T, Forland EJ, Roald LA (2008) Climate change impacts on hydrological processes in Norway based on two methods for transferring regional climate model results to meteorological station sites. *Tellus, Ser A Dyn Meteorol Oceanogr* 60 A:439–450. doi:10.1111/j.1600-0870.2008.00306.x
- Biasutti M, Sobel AH (2009) Delayed Sahel rainfall and global seasonal cycle in a warmer climate. *Geophys Res Lett*. doi:10.1029/2009GL041303
- Bierkens MFP (2015) Global hydrology 2015: state, trends, and directions. *Water Resour Res* 51:4923–4947. doi:10.1002/2015WR017173
- Cornelissen T, Diekkötter B, Giertz S (2013) A comparison of hydrological models for assessing the impact of land use and climate change on discharge in a tropical catchment. *J Hydrol* 498:221–236. doi:10.1016/j.jhydrol.2013.06.016
- Dettinger MD, Diaz HF (2000) Global characteristics of stream flow seasonality and variability. *J Hydrometeorol* 1:289–310. doi:10.1175/1525-7541(2000)001<0289:GCOSFS>2.0.CO;2
- Döll P, Fiedler K, Zhang J (2009) Global-scale analysis of river flow alterations due to water withdrawals and reservoirs. *Hydrol Earth Syst Sci* 13:2413–2432. doi:10.5194/hessd-6-4773-2009
- Gelfan A, Gustafsson D, Motovilov Y et al (2016) Climate change impact on water regime of great Arctic rivers: modeling and uncertainty issues. *Clim Chang*. doi:10.1007/s10584-016-1710-5
- Greuell W, Andersson JCM, Donnelly C et al (2015) Evaluation of five hydrological models across Europe and their suitability for making projections under climate change. *Hydrol Earth Syst Sci Discuss* 12:10289–10330. doi:10.5194/hessd-12-10289-2015
- Grill G, Lehner B, Lumsdon AE et al (2015) An index-based framework for assessing patterns and trends in river fragmentation and flow regulation by global dams at multiple scales. *Environ Res Lett* 10:15001. doi:10.1088/1748-9326/10/1/015001
- Haddeland I, Heinke J, Biemans H et al (2014) Global water resources affected by human interventions and climate change. *Proc Natl Acad Sci U S A* 111:3251–3256. doi:10.1073/pnas.1222475110
- Hagemann S, Chen C, Clark DB et al (2013) Climate change impact on available water resources obtained using multiple global climate and hydrology models. *Earth Syst Dyn* 4:129–144. doi:10.5194/esd-4-129-2013
- Hawkins E, Sutton R (2009) The potential to narrow uncertainty in regional climate predictions. *Bull Am Meteorol Soc* 90:1095–1107. doi:10.1175/2009BAMS2607.1
- Hempel S, Frieler K, Warszawski L et al (2013) A trend-preserving bias correction &ndash; the ISI-MIP approach. *Earth Syst Dynam* 4:219–236. doi:10.5194/esd-4-219-2013
- Huang S, Kumar R, Flörke M et al (2016) Evaluation of an ensemble of regional hydrological models in 12 large-scale river basins worldwide. *Climatic Change*. doi:10.1007/s10584-016-1841-8
- Jung IW, Bae DH, Lee BJ (2013) Possible change in Korean streamflow seasonality based on multi-model climate projections. *Hydrol Process* 27:1033–1045. doi:10.1002/hyp.9215
- Krylenko I, Motovilov Y, Antokhina E et al (2015) Physically-based distributed modelling of river runoff under changing climate conditions. *IAHS Publ* 368:156–161. doi:10.5194/piahs-368-156-2015
- Lee J-Y, Wang B (2012) Future change of global monsoon in the CMIP5. *Clim Dyn* 42:101–119. doi:10.1007/s00382-012-1564-0
- Menon A, Levermann A, Schewe J et al (2013) Consistent increase in Indian monsoon rainfall and its variability across CMIP-5 models. *Earth Syst Dyn* 4:287–300. doi:10.5194/esd-4-287-2013
- Morán-Tejeda E, Lorenzo-Lacruz J, López-Moreno JI et al (2014) Streamflow timing of mountain rivers in Spain: recent changes and future projections. *J Hydrol* 517:1114–1127. doi:10.1016/j.jhydrol.2014.06.053
- Patricola CM, Cook KH (2010) Sub-Saharan northern African climate at the end of the twenty-first century: forcing factors and climate change processes. *Clim Dyn* 37:1165–1188. doi:10.1007/s00382-010-0907-y
- Patterson LA, Lutz B, Doyle MW (2013) Climate and direct human contributions to changes in mean annual streamflow in the South Atlantic, USA. *Water Resour Res* 49:7278–7291. doi:10.1002/2013WR014618



- Prudhomme C, Giuntoli I, Robinson EL et al (2014) Hydrological droughts in the twenty-first century, hotspots and uncertainties from a global multimodel ensemble experiment. *Proc Natl Acad Sci U S A* 111:3262–3267. doi:[10.1073/pnas.1222473110](https://doi.org/10.1073/pnas.1222473110)
- Samaniego L, Kumar R, Breuer L et al (2016) Propagation of forcing and model uncertainties on to hydrological drought characteristics in a multi-model century-long experiment in large river basins. *Climatic Change*. doi:[10.1007/s10584-016-1778-y](https://doi.org/10.1007/s10584-016-1778-y)
- Schewe J, Heinke J, Gerten D et al (2014) Multimodel assessment of water scarcity under climate change. *Proc Natl Acad Sci U S A* 111:3245–3250. doi:[10.1073/pnas.1222460110](https://doi.org/10.1073/pnas.1222460110)
- Schneider C, Laizé CLR, Acreman MC, Flörke M (2013) How will climate change modify river flow regimes in Europe? *Hydrol Earth Syst Sci* 17:325–339. doi:[10.5194/hess-17-325-2013](https://doi.org/10.5194/hess-17-325-2013)
- Vano JA, Nijssen B, Lettenmaier DP (2015) Seasonal hydrologic responses to climate change in the Pacific northwest. *Water Resour Res* 51:1959–1976. doi:[10.1002/2014WR015909](https://doi.org/10.1002/2014WR015909)
- Vetter T, Reinhardt J, Flörke M et al (2016) Evaluation of sources of uncertainty in projected hydrological changes under climate change in 12 large-scale river basins. *Climatic Change*. doi:[10.1007/s10584-016-1794-y](https://doi.org/10.1007/s10584-016-1794-y)
- Vetter T, Huang S, Aich V et al (2015) Multi-model climate impact assessment and intercomparison for three large-scale river basins on three continents. *Earth Syst Dyn* 6:17–43. doi:[10.5194/esd-6-17-2015](https://doi.org/10.5194/esd-6-17-2015)
- Wada Y, Wisser D, Eisner S et al (2013) Multimodel projections and uncertainties of irrigation water demand under climate change. *Geophys Res Lett* 40:4626–4632. doi:[10.1002/grl.50686](https://doi.org/10.1002/grl.50686)
- Walsh RP, Lawler DM (1981) Rainfall seasonality: description, spatial patterns and change through time. *Weather* 36:201–208. doi:[10.1002/j.1477-8696.1981.tb05400.x](https://doi.org/10.1002/j.1477-8696.1981.tb05400.x)
- Wang D, Hejazi M (2011) Quantifying the relative contribution of the climate and direct human impacts on mean annual streamflow in the contiguous United States. *Water Resour Res*. doi:[10.1029/2010WR010283](https://doi.org/10.1029/2010WR010283)
- Warszawski L, Frieler K, Huber V et al (2014) The inter-sectoral impact model intercomparison project (ISI-MIP): project framework. *Proc Natl Acad Sci U S A* 111:3228–3232. doi:[10.1073/pnas.1312330110](https://doi.org/10.1073/pnas.1312330110)